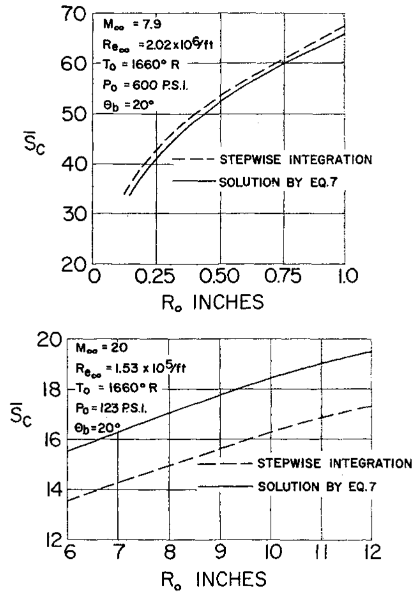

Fig. 2 Swallowing distance $\bar{s}_c$ as a function of the nose radius

stepwise integration is presented in Fig. 2. It is seen in the first example that the results from Eq. (7) are in good agreement with those obtained by stepwise integration of Eq. (3). However, in the second case, where the freestream Mach number is comparatively low, the difference is of the order of 15%.

By means of the linearized relation for $\bar{s}_c$, it also is possible to make an estimate of the transition point when the transition Reynolds number, based on the momentum thickness, is known:

$$Re_\theta \cong \left\{\frac{p_c}{6\lambda\,(R/\lambda)^{1/2}T_0}\left[3(M_c - M_s)\,\frac{\bar{s}}{\bar{s}_c} + M_s\right] \times \left(1 + \frac{\gamma - 1}{2}\,M_e^2\right) R_0\bar{s}\right\}^{1/2} \int_0^{\eta_e} f'(1 - f')d\eta \qquad (8)$$

The transition Reynolds number predicted by Eq. (8) is in fairly good agreement with the experimental data of Ref. 4. The numerical values are listed in Table 1.

In addition to this comparison, the transition points also were calculated for the conditions as given in Fig. 1, assuming that transition occurs when $Re_\theta = 700$. This result has been obtained for a blunted cone with $R_0 = 0.2$ and $\theta = 15°$ under nearly the same freestream conditions as are presented in Ref. 2.

As mentioned in the foregoing, the dependence of the external flow properties on the nose radius vanishes when they are expressed in terms of the similarity parameter of Ref. 2. This is shown in Fig. 3, where the Mach number variation obtained by the present analysis is compared to the experimental data of Ref. 4.

Table 1

Experimental data (Ref. 4)			Present analysis	
R_0, in.	$\bar{x}_{trans}$	$Re_{\theta trans}$	$Re_{\theta trans}$	$M_{e trans}$
0.0480	115	620	660	3.30
0.0830	55	550	490	2.71
0.1650	39	?	460	2.58
0.4900	12	?	385	2.35

References

[1] Ferri, A. and Libby, P. A., "Note on an interaction between the boundary layer and the inviscid flow," J. Aeronaut. Sci. **21**, 130 (1954).

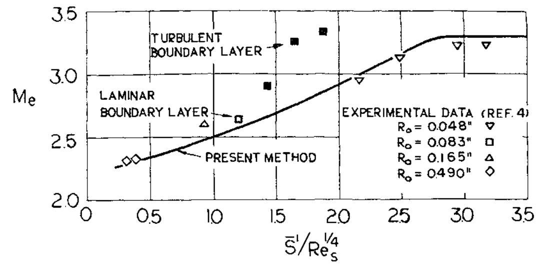

Fig. 3 Similarity parameter for similar blunt bodies; $M_\infty = 3.81$, $T_0 = 560°R$, $\theta_b = 7.5°$

[2] Ferri, A., "Some heat transfer problems in hypersonic flow," *Aeronautics and Astronautics* (Pergamon Press, New York, 1960), pp. 344–377.

[3] Lees, L., "Laminar heat transfer over blunt-nosed bodies at hypersonic flight speeds," Jet Propulsion 26, 259–269 (1956).

[4] Rogers, R. H., "Boundary layer development in supersonic shear flow," AGARD Rept. 269 (April 1960).

[5] Zakkay, V. and Krause, E., "Boundary conditions at the outer edge of the boundary layer on blunted conical bodies," Polytechnic Inst. Brooklyn, PIBAL Rept. 747, ARL 62-386 (July 1962).

Integral Method Solutions of Laminar Viscous Free-Mixing

M. H. Steiger* and M. H. Bloom†
Polytechnic Institute of Brooklyn, Farmingdale, N. Y.

Introduction

The integral method furnishes a convenient means for the study of nonsimilar boundary-layer problems such as in viscous free-mixing. This paper deals with laminar, two-dimensional, symmetric and axisymmetric, incompressible, uniform pressure wakes and jets. Solutions are derived by using the simple one-strip integral method and are presented in closed form. It is shown that the present theory agrees reasonably well with other more accurate, but very cumbersome, methods of solution. Compressibility, turbulence, thermal, and other diffusive properties can be studied by analogous means.

Analysis

The following boundary-layer equations are assumed to govern the viscous free-mixing previously discussed and represented schematically in Fig. 1:

Continuity

$$u_x + v_y + \epsilon(v/y) = 0 \qquad (1)$$

Momentum

$$uu_x + vu_y = \nu[u_{yy} + \epsilon(u_y/y)] \qquad p = \text{const} \qquad (2)$$

where $\epsilon = 0, 1$ for two-dimensional and axisymmetric flow, respectively; x and y are the streamwise and normal coordinates with velocity components u and v; p denotes pressure; ν kinematic viscosity; and subscripts x and y denote partial differentiation with respect to the indicated variable.

Received March 18, 1963. The study was supported partially by the Air Force Office of Scientific Research Grant AF-AFOSR-1-63.

* Research Associate, Graduate Center. Member AIAA.
† Professor, Aerospace Engineering, Graduate Center. Member AIAA.

Table 1

Case	Profile	$\left(\dfrac{d^2f}{dn^2}\right)_0$
1	$f(n^2) = n^2$	2
2	$f(n^2) = 2n^2 - n^4$	4
3	$f(n^2) = 3n^2 - 3n^4 + n^6$	6
4	$f(n^2) = 4n^2 - 6n^4 + 4n^6 - n^8$	8

The appropriate boundary conditions are

$$\text{at } y = 0 \qquad u_y = v = 0 \tag{3a}$$

and

$$\text{at } y = \delta \qquad u = u_e = \text{const} \tag{3b}$$

where δ is the viscous layer thickness (i.e., the distance from the symmetric axis, $y = 0$, to the value of y when $u \cong 0.995u_e$), and subscript e denotes conditions at the edge of the viscous layer.

By using well-known operations, the following integral equation and boundary condition along the x axis are derived:

$$\delta^{1+\epsilon} \int_0^1 \bar{u}(1 - \bar{u})n^\epsilon dn = \theta_c = \text{const} \tag{4}$$

and

$$\bar{u}_0(d\bar{u}_0/ds) = 2^\epsilon[\theta_c^{2-\epsilon}/\delta^2]\bar{u}_{nn_0} \tag{5}$$

where $n = y/\delta$, $s = \nu_e(x - x_c)/u_e\theta_c^{2-\epsilon}$, $\bar{u} = u/u_e$, $\bar{u}_{nn} = \partial^2\bar{u}/\partial n^2$, and subscripts c and 0 denote conditions at an initial station and variables evaluated along the x axis (i.e., at $y = 0$), respectively.

The assumed profile is defined by

$$\bar{u} = \bar{u}_0 + (1 - \bar{u}_0)f(n^2) \tag{6}$$

where $\bar{u}_0$ denotes u/u_e at $y = 0$, and $f(n^2)$ is a function of n^2.

With (6), Eqs. (4) and (5) are solved readily in closed form. The solution for two-dimensional flow is given by

$$(x - x_c) = (u_e\theta_c^2/\nu_e)\beta[F(\bar{u}_0) - F(\bar{u}_{0c})] \tag{7a}$$

where

$$F(\bar{u}_0) = \frac{2B(2A - B)\bar{u}_0^2 + (2A - B)(A - 3B)\bar{u}_0 + A(5B - A)}{2(A + B)(1 - \bar{u}_0)^2(A + B\bar{u}_0)} + \frac{B(B - 2A)}{(A + B)^2} \ln\left(\frac{A + B\bar{u}_0}{1 - \bar{u}_0}\right) \tag{7b}$$

The constants A and B only depend on the functional form of $f(n^2)$, namely,

$$A = \int_0^1 f(1 - f)dn \qquad B = \int_0^1 (1 - f)^2 dn$$

and $\beta = [(A+B)^2(d^2f/dn^2)_0]^{-1}$.

It is of interest to note that as

$$\bar{u}_0 \to 1.0 \text{ (i.e., } u_0 \to u_e) \qquad F(\bar{u}_0) = 1/2(1 - \bar{u}_0)^2 \tag{7c}$$

For axisymmetric free-mixing the solution is

$$x - x_c = (u_e\theta_c/\nu_e)\kappa[G(\bar{u}_0) - G(\bar{u}_{0c})] \tag{8a}$$

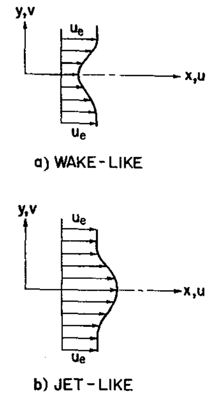

Fig. 1 Schematic of axial section of free-mixing flow

where

$$G(\bar{u}_0) = \frac{1}{1 - \bar{u}_0} - \frac{C}{C + D}\ln\left(\frac{C + D\bar{u}_0}{1 - \bar{u}_0}\right) \tag{8b}$$

$$C = \int_0^1 f(1 - f)ndn \qquad D = \int_0^1 (1 - f)^2 ndn$$

$$\kappa = \left[(C + D)\left(\frac{d^2f}{dn^2}\right)_0\right]^{-1}$$

and noting that as

$$\bar{u}_0 \to 1.0 \qquad G(\bar{u}_0) = 1/1 - \bar{u}_0 \tag{8c}$$

Tables 1, 2, and 3 list some typical profiles and their associative constants.

Table 2

Case	A	B	β	C	D	κ
1	0.13333	0.53333	1.12500	0.08333	0.16667	2.000
2	0.12698	0.40635	0.87892	0.06667	0.10000	1.500
3	0.11615	0.34099	0.79752	0.05357	0.07143	1.333
4	0.10782	0.29954	0.75330	0.04444	0.05556	1.250
5,6	...	...	0.63662	...	...	1.000

Cases 5 and 6 correspond to the exact downstream asymptotic solution for two-dimensional and axisymmetric flow, respectively.

It is only meaningful to compare wakes with equal drag and, therefore, with equal initial momentum thickness. It is of interest to note that for equal drag wakes Eqs. (7) and (8) show that the streamwise scale, as $\bar{u}_0 \to 1$, is only influenced by the constants β and κ, which in turn only depend on the functional form of $f(n^2)$. Some representative numerical values of β and κ are given in Table 2 for various profiles.

In Table 3 the present theory for two-dimensional flow is compared with the numerical solution given by Goldstein[1] and the four-strip integral method (Pallone and Erdos, Fig. 3 of Ref. 2).

Table 3 Two-dimensional flow

	$x(u_e\theta_c^2/\nu_e)$		
u_0/u_e	Present theory, case 4	Goldstein[1]	Pallone, four-strip integral method[2]
0	0	0	0
0.123	0.070	0.009	...
0.359	0.592	0.245	...
0.560	1.886	1.134	0.940
0.650	3.238	2.268	1.816
0.773	8.062	6.350	4.900
0.900	40.491	30.618	25.600
0.990	3802.000	3184.000	2600.000
		Blasius initial profile	

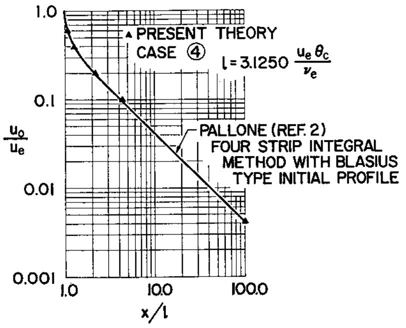

Fig. 2 Velocity decay along axis of incompressible axisymmetric wake

In Fig. 2, a comparison for an axisymmetric wake is made between the present theory and the four-strip integral method (Fig. 4 of Ref. 2). The solution presented in Ref. 2 is plotted in terms of x/l, where l is a constant characteristic length. In Ref. 2 a relation exists between l and the drag of the body, and therefore $(u_e\theta_c/\nu_e)$ is not given. However, the relationship can be calculated from the asymptotic solution [Eq. (8c)] $x = (u_e\theta_c/\nu_e)\kappa(1 - \bar{u}_0)^{-1}$ by taking from Fig. 4 of Ref. 2 asymptotic values of x and $\bar{u}_0$, namely, $x = 100$ when $1 - \bar{u}_0 = 0.004$. This yields $l = 2.5\kappa(u_e\theta_c/\nu_e)$. The present theory then is extrapolated upstream by using Eq. (8a).

References

[1] Goldstein, S., "On the two-dimensional steady viscous fluid behind a solid body," Proc. Roy. Soc. (London) **A142**, 545 (1933).

[2] Pallone, A. and Erdos, J., "Hypersonic laminar wakes and transition studies," Avco Corp., Wilmington, Mass., Tech. Memo. RAD-TM-62-104 (January 1963).

Classical Analog of the Photoelectric Effect

J. G. Logan*
Aerospace Corporation, Los Angeles, Calif.

Based on the analyses of Grad and Lees, the rarefied gas field recently has been shown to possess the unique characteristic that small plane longitudinal and transverse disturbances can propagate within the field.[1–6] Small momentum and energy disturbances produced by impulsive boundary motions cannot be confined to regions near the boundary and can propagate over very large distances in the field before being damped by collisions. This disturbance propagation occurs when the relaxation time is very large and the particle density is very small ($<10^{10}$ particles per unit volume).

If an infinite plate undergoes a small impulsive motion $U(U \ll c)$ in a direction normal to its surface, the disturbance motion produced in a rarefied gas field initially in equilibrium can be described by the linearized one-dimensional longitudinal propagation equations previously derived.[4] If specular reflection does not occur at the boundary and the plate is in thermal equilibrium with the field at temperature T_0, the field particles that collide with the plate can be assumed to be absorbed and re-emitted at equilibrium conditions (p_0, T_0) with a velocity U(Fig. 1). During the impulsive plate motion, the average mass flow $\rho_0\bar{c}$ approaching the plate, boundary A, where $\bar{c}$ is an average random particle velocity, is increased upon re-emission to $\rho_0(\bar{c} + U)$. The characteristic propagating quantities at boundary A become $P_{1\pm} = \mp 0.42U/c_0$, $P_{2\pm} = \pm 1.66U/c_0$.

When these disturbances impinge upon a stationary boundary B, also at temperature T_0, the slow and fast characteristics yield an average disturbance pressure $p = 1.29U/c_0$ at point 1 and $p = 1.61U/c_0$ at point 2. The pressure produced by the longitudinal disturbance is directly proportional to the disturbance velocity. If the disturbances impinge on a free body of mass M_0 and sufficient collisions occur to impart a velocity U (the maximum disturbance velocity that can be imparted, since $p = p_0$ when $u_w = U$), the free body can acquire a maximum momentum $M_p = M_0U$ and a maximum energy $E_0 = \frac{1}{2}M_0U^2$.

Physically, the process of momentum and energy transfer occurs by individual field particle collisions. Momentum and energy are imparted to the field particles at the boundary A, and the field particles transfer momentum and energy directly to the body B. The transfer process can be idealized by assuming that the field particle of mass m_0 possesses, after the disturbance motion is imparted to the field particle at the boundary, an average velocity $(\bar{c} + U)$, an average energy $\frac{1}{2}m_0(\bar{c} + U)^2$, and an average momentum $m_0(\bar{c} + U)$. If n_0 collisions are required to produce a maximum velocity U of the free body of mass M_0, then the maximum momentum M_p and maximum energy E_0 transferred are given by

$$M_p = n_0[m_0(\bar{c} + U) - m_0\bar{c}] = n_0m_0U = M_0U \tag{1a}$$

$$E_0 = \alpha n_0[\tfrac{1}{2}m_0(\bar{c} + U)^2 - \tfrac{1}{2}m_0\bar{c}^2] \approx \alpha n_0m_0\bar{c}U = \tfrac{1}{2}M_0U^2 \tag{1b}$$

where α is the relative efficiency of energy transfer, $2\alpha = U/c$. On the average, n_0 collisions will occur in a direction opposite to the motion by particles with an average velocity $\bar{c}$.

The momentum and energy transferred are directly proportional to the amplitude of the disturbance motion. If the impulsive boundary motion of duration t_0 occurs over a fixed distance r_0, $U = r_0/t_0$ and the maximum energy E_0 transferred by the collisions is inversely proportional to the duration, i.e., $E_0 \sim 1/t_0$, or directly proportional to a frequency factor $\omega_0 = 1/t_0$.

An increase in the field density or field intensity, i.e., an increase in the number of boundary collisions per unit time, will not alter the maximum value E_0. A change in the field intensity only will alter the time interval $\Delta t \leqslant t_0$ in which a given value of energy can be imparted to the body, i.e., an uncertainty relation can be defined by

$$\Delta E\, \Delta t \leqslant E_0\, t_0 = \text{const}$$

which is related to the statistical collision process for the acquisition of the small excess energy $\Delta E \leqslant E_0$.

This process of energy transfer in a rarefied gas field is remarkably similar to the energy transfer process described by the photoelectric effect. If the energy transferred by n_0 field

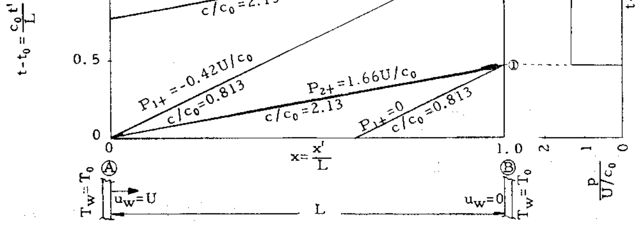

Fig. 1 Characteristic disturbance generated by normal impulsive motion of an infinite plate in a very rarefied gas field

Received March 22, 1963.

* Director, Aerodynamics and Propulsion Research Laboratory. Member AIAA.